M. E. Debakey, *Artif. Org.* **7**, 31 (1983); D. Gospodarowicz, I. Vlodavsky, N. Savion, *J. Supramol. Struct.* **13**, 339 (1980); P. A. Jones, *Proc. Natl. Acad. Sci. U.S.A.* **76**, 1882 (1979).
4. E. Bell, B. Ivarsson, C. Merrill, *Proc. Natl. Acad. Sci. U.S.A.* **76**, 1274 (1979); E. Bell, H. P. Erlich, D. J. Buttle, T. Nakatsuji, *Science* **211**, 1052 (1981); C. B. Weinberg and E. Bell, *J. Cell. Physiol.* **122**, 410 (1985).
5. C. B. Weinberg and E. Bell, *J. Cell Biol.* **99**, 66A (1984).
6. For most experiments, the mold was a 25-mm test tube with a 6-mm polished glass mandrel, although models have been made with internal diameters from 2 mm to 1 cm. The standard model, 7.5 cm long, was made with a mixture of 13.8 ml of 1.76× McCoy's 5A medium supplemented with antibiotics and 2.7 ml of fetal bovine serum (Flow Laboratories or Gibco Laboratories), 1.5 ml of 0.1*N* NaOH, 9.0 ml of porcine skin collagen (produced by Pentapharm A.G. and kindly provided by Centrechem) or rat tail tendon collagen dissolved at 3.2 to 3.4 mg/ml in 0.1 percent acetic acid, and 3.0 ml of culture medium containing 5×10^5 smooth muscle cells per milliliter.
7. B. Nusgens, C. Merrill, C. Lapierre, E. Bell, *Collagen Rel. Res.* **4**, 351 (1984); D. E. Birk and R. L. Trelstad, *J. Cell Biol.* **99**, 2024 (1984).
8. L. W. Hoyer, R. P. de los Santos, J. R. Hoyer, *J. Clin. Invest.* **52**, 2737 (1973); E. A. Jaffe, L. W. Hoyer, R. L. Nachman, *J. Clin. Invest.* **52**, 2757 (1973).
9. S. Bunting, R. Grygleski, S. Moncada, J. R. Vane, *Prostaglandins* **12**, 897 (1976); B. B. Weksler, A. J. Marcus, E. A. Jaffe, *Proc. Natl. Acad. Sci U.S.A.* **74**, 3922 (1977).
10. A. Eldor, D. J. Falcone, D. P. Hajjar, C. R. Minick, B. B. Weksler, *J. Clin. Invest.* **67**, 735 (1981); A. Eldor *et al.*, *J. Cell Physiol.* **114**, 179 (1983).
11. U. Delvos, C. Gajdusek, H. Sage, L. A. Harker, S. M. Schwartz, *Lab. Invest.* **46**, 61 (1982).
12. The optimized models had three layers of collagen and cells alternating with two meshes (1×10^5 cells and 1.5 mg of collagen per milliliter were used in the casting mixture) and had been aged for 1 month in vitro.
13. D. Faustman, V. Hauptfeld, P. Lacy, J. Davie, *Proc. Natl. Acad. Sci. U.S.A.* **78**, 5156 (1981); K. J. Lafferty, A. Bootes, G. Part, D. W. Talmage, *Transplantation* **22**, 138 (1976); H. Lau, K. Reemsta, M. A. Hardy, *Science* **221**, 754 (1983); S. E. Sher, B. E. Hull, S. Rosen, D. Church, L. Friedman, E. Bell, *Transplantation* **36**, 552 (1983).
14. We thank L. D. Honaryar, C. Merrill, and H. Youssoufian for culturing cells, and H. Moore for histological assistance. We are grateful to H. B. Haimes for performing the electron microscopy, which was carried out with the assistance of E. Hartwieg of the Department of Biology Electron Microscope Facility, Massachusetts Institute of Technology

28 June 1985; accepted 23 October 1985

Sevenless: A Cell-Specific Homeotic Mutation of the *Drosophila* Eye

ANDREW TOMLINSON AND DONALD F. READY

Each ommatidium in the compound eye of the *Drosophila* mutant *sevenless* lacks photoreceptor number seven (R7) from the normal ommatidial complement of eight photoreceptors. A comparison of mutant and normal development reveals that this deficit is caused by the cell-specific transformation of the cell normally fated to produce R7 into a lens-secreting accessory cell, a cone cell.

DURING DEVELOPMENT, CELLS SELECT pathways of specialization that lead to the differentiation of particular cell types. Disturbances of this selection process can lead to the substitution of a normal pattern element with one appropriate to another location; the term homeosis was introduced to describe this condition (*1*). For example, in *Drosophila* the homeotic mutation *bithorax* directs cells normally destined to differentiate metathoracic structures to produce their mesothoracic counterparts (*2*). We studied compound eye development in the *Drosophila* mutant *sevenless* (*3*), in which each ommatidium lacks photoreceptor number seven (R7) from the normal ommatidial complement of eight photoreceptors (*4, 5*). In the developing mutant ommatidium, a cell occupies the site normally taken by the prospective R7 cell. Instead of becoming a photoreceptor, however, the cell differentiates into a lens-secreting cone cell. Thus *sevenless* is a cell-specific homeotic mutation, precisely switching the developmental fate of one cell to that of another.

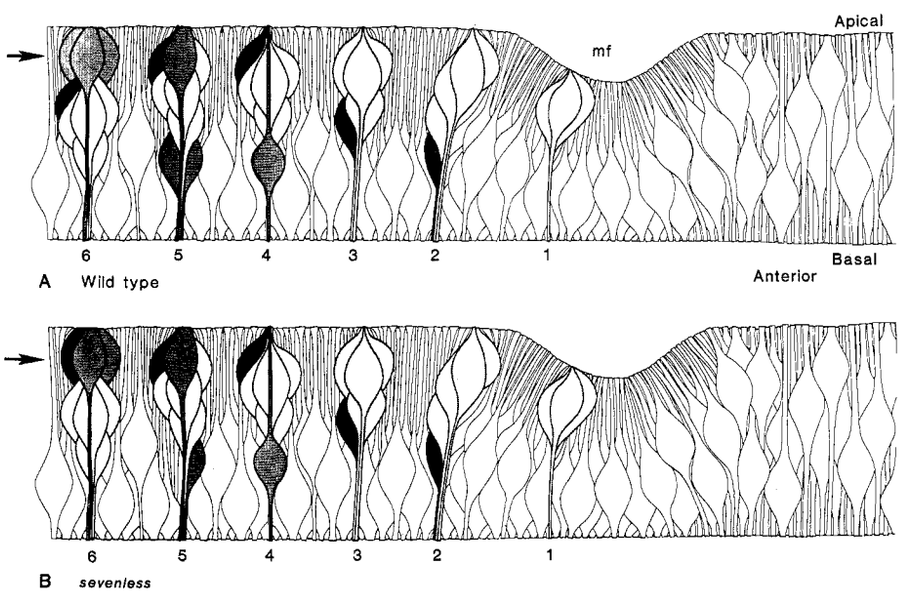

Fig. 1. Schematic side view of ommatidial assembly in wild type (A) and *sevenless* (B) (not all precursor cells shown). All cells (except for dividing cells, not shown) extend from the apical surface to the basement membrane of the epithelium. The nuclei are located in the cell bodies. Photoreceptor R7, black; cone cells, dark gray; photoreceptors R1 to R6 and R8, light gray; all other cells, white; and mf, morphogenetic furrow. Arrows indicate plane of sections shown in Fig. 2. (A) Region 1 comprises a five-cell precluster. In region 2, R1, R6, and R7 rise to join the precursor. Region 3 contains a symmetrical cluster. In region 4, as R7 completes apical migration, two cone cell nuclei rise. In region 5 two more cone cell nuclei rise. In region 6 four cone cell nuclei overlie the photoreceptors. (B) Regions 1, 2, 3, and 4 are as described in (A). In region 5 only a single cone cell nucleus rises. In region 6 the cell in the R7 position remains apical and joins the cone cell unit; only seven photoreceptors sink basally.

The developing compound eye of *Drosophila* is well suited to an examination of pathway selection at the level of individual cells. Each of the approximately 750 ommatidia that comprise the compound eye is a stereotyped cellular assembly in which every cell can be identified by its unique position. This architectural stereotypy applies also to the developing ommatidia, permitting the fate of a cell to be read from its characteristic position as it joins the assembly (*6, 7*).

The compound eye grows by the sequential addition of new ommatidial precursors to its anterior margin (*8*); anterior ommatidia are younger than posterior ones. Since each ommatidial precursor is slightly more developed than its anterior neighbor, a maturational gradient is laid out spatially along the anterior-posterior axis of the epithelium. Electron microscopic reconstruction of a series of precursors lying along the maturational axis thus reveals the smooth progression of stages through which an individual

Department of Biology, Princeton University, Princeton, NJ 08540.

ommatidium passes during assembly (*7*).

The retinal epithelium is a monolayer in which all cells extend from the apical surface to the basement membrane (Fig. 1). Ommatidia assemble within this epithelium in a carefully orchestrated program of nuclear movements. Ahead of a distinct furrow across the epithelium, cells are unpatterned and their nuclei are distributed uniformly throughout the depth of the monolayer. In the center of the furrow, nuclei sink basally, leaving the apical reaches of the epithelium devoid of nuclei. Ommatidial assembly then commences as five nuclei move apically to form a stereotyped precluster of photoreceptors R2, R3, R4, R5, and R8 (region 1 in Fig. 1A). Cells surrounding the preclusters then undergo a final division and generate a basal pool of nuclei below the preclusters (*6, 7*).

Ommatidial construction continues as nuclei rise from the basal pool and are incorporated into precise apical positions within the precursor. Shortly after the postfurrow mitoses, the photoreceptor octet is completed by the sequential upward movement of the nuclei of R6, R1, and R7 (region 2 in Fig. 1A), forming a bilaterally symmetrical cluster of eight neurons (region 3 in Figs. 1A and 2A). A bundle of eight axons emerges from each symmetrical cluster and enters the optic stalk (Fig. 2A). At this stage the nucleus of R7 is still rising; it has segregated from the basal pool of nuclei but is still below the nuclei of the other photoreceptors (region 3 in Fig. 1A). As the nucleus of R7 completes its apical migration, two nuclei emerge from the basal pool and rise to flank the cluster (regions 4 and 5 in Fig. 1A). These are the nuclei of two of the four cone cells that will secrete the ommatidial lens during pupal life. The photoreceptor cluster now begins to sink into the epithelium and two more cone cell nuclei join the apical pair (regions 5 and 6 in Fig. 1A). This nuclear choreography establishes the essential ommatidial architecture: a quartet of lens-secreting cone cells is positioned above the eight photoreceptors (*6, 7*).

Before the apical migration of their nuclei, photoreceptors R1, R6, and R7 can be identified by the contacts they make with the photoreceptors already incorporated into the precluster. These contacts are maintained throughout the depth of the epithelium, and each of the cells is positioned in a unique niche in the developing ommatidium. Shortly after it is generated in the final round of cell divisions, the cell destined to form R7 can be identified as the occupant of the niche whose walls are formed by R6, R8, and R1 (*7*). This niche and its occupant at the symmetrical cluster stage are shown in Fig. 2A.

Reconstruction of the developmental program in *sevenless* through electron microscopy of serial thin sections revealed that the symmetrical cluster was established in a normal manner (regions 1 to 3 in Fig. 1B) and that the R7 niche was filled in characteristic fashion (Fig. 2B). However, the cell in the R7 position failed to produce an axon and a bundle of only seven axons projected into the optic stalk (Fig. 2B); this was the first morphologically detectable aberration in the mutant. The nucleus of the cell in the R7 niche continued to behave normally, completing its apical migration as the first pair of cone cell nuclei rose (regions 4 and 5 in Fig. 1B). But when the photoreceptor cluster began to sink into the epithelium, the nucleus of the cell in the R7 niche did not move back down, remaining instead in the most apical regions of the epithelium with the two cone cell nuclei. A single nucleus now moved up from the basal pool on the side of the cluster opposite the R7 niche to complete the apical four-cell unit (regions 5 and 6 in Figs. 1B and 2D). This quartet subsequently behaved as a typical cone cell group. This behavior was seen consistently in over 100 developing *sevenless* ommatidia sampled from five serially sectioned epithelia; similar transformations were observed

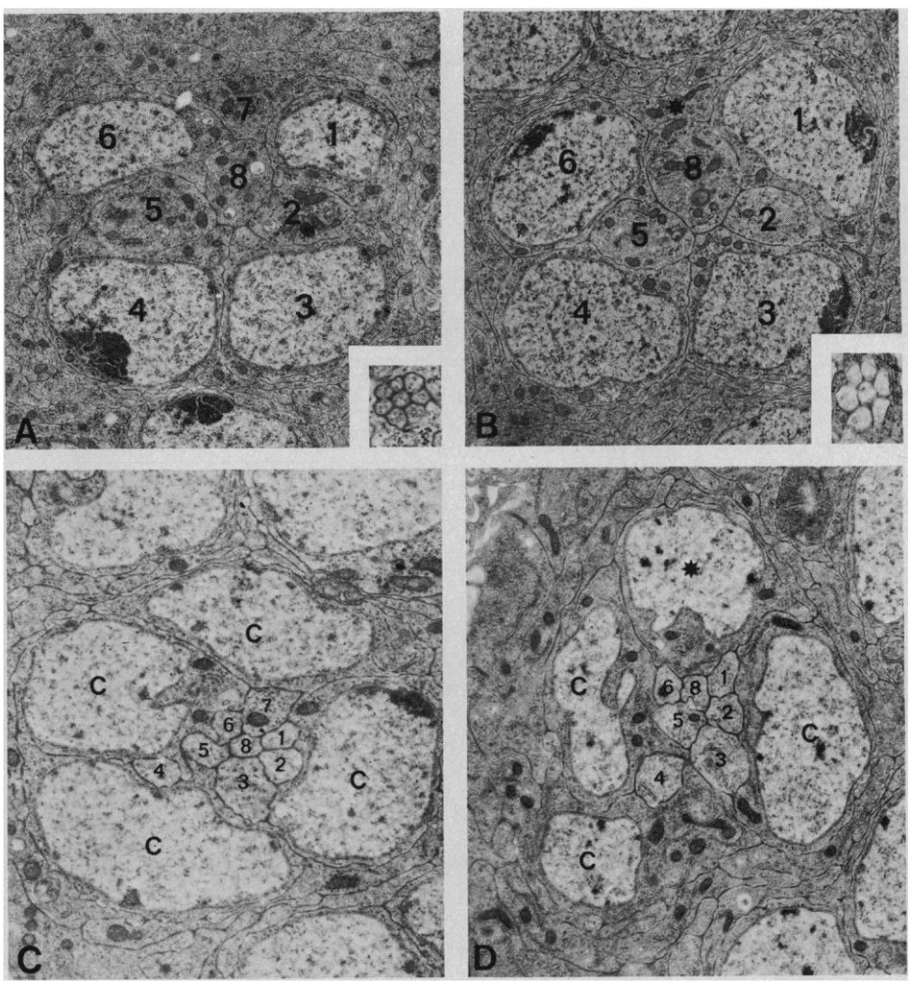

Fig. 2. Electron micrographs of thin sections through wild-type (A and C) and *sevenless* (B and D) late third-instar eye disks. Fixation and processing of the tissue were performed as described by Tomlinson (*7*). (A) Section through the apical region of a wild-type bilaterally symmetrical cluster. Photoreceptor cells are numbered. The nuclei of R1, R3, R4, and R6 are evident; those of R2, R5, and R8 are found slightly below this level; and that of R7 is more deeply placed. R7 contacts R1, R6, and R8 throughout the entire depth of the epithelium. A bundle of eight axons (inset) emerges basally from the cluster and enters the optic stalk. (B) Section through the symmetrical cluster found in *sevenless*. The R7 niche is occupied (asterisk). Note that the cell contacts R1, R6, and R8; these contacts are maintained throughout the depth of the epithelium. Details are as described in (A) except that a bundle of only seven axons (inset) enters the optic stalk. (C) Section through apical quartet of cone cells (c). Apical projections from the underlying photoreceptors are numbered. (D) Section through the same stage as in (C) in *sevenless*. The nucleus from the R7 niche in (B) (asterisk) has risen and has been integrated into the cone cell clustering. Note the absence of the R7 apical projection and the photoreceptor contacts (R1, R6, and R8) made by the transformed cell (asterisk). All magnifications ×8000.

in three additional *sevenless* alleles (*3*).

In an earlier study (*5*), it was suggested that the presumptive R7 cell was absent from the developing *sevenless* ommatidium. This interpretation may have been based on the appearance of stages equivalent to that represented in Fig. 2D, when the transformation has already taken place.

Drosophila eye cells are directed into their developmental pathways by environmental cues rather than by cell lineage (*6, 9*), and a cell occupying the R7 niche is normally fated to become R7. It is not known whether a mutant cell attempts to become R7 but defaults into the cone cell pathway or whether the mutation specifically orders an uncommitted cell into the cone cell pathway. The cell in the R7 niche displays the characteristic dynamics of R7 until comparatively late in the nuclear choreography, but as early as the symmetrical cluster stage the absence of an axon indicates it has deviated from the photoreceptor pathway.

The cell occupying the R7 niche in *sevenless* appears to be developmentally misdirected by an intrinsic defect rather than by an abnormal cellular environment. Mosaic eyes composed of a mixture of normal and *sevenless* cells (marked with the pigment-deleting mutation *white*) do not contain *white* R7 cells (*4, 5*); normal surrounding cells are unable to rescue a mutant cell in the R7 position. Conversely, pigmented R7 cells can be found in otherwise *white*, and thus genetically *sevenless*, ommatidia, indicating that surrounding mutant cells cannot pull a normal R7 cell into mutant behavior (*4, 5*). The cell in the R7 niche thus appears to receive the correct developmental cues but is unable to respond appropriately. This cell-autonomous action of *sevenless* is distinct from the "transfating" observed in the leech and nematode, in which a changed cellular environment can cause a cell to switch its fate (*10, 11*).

In the mutant, an "extra" nucleus does not emerge from the basal pool and display recognizable cone cell behavior. Thus we cannot yet tell if a redundant cone cell is never elicited in the mutant retinal epithelium or if a presumptive cone cell is developmentally redirected or dies. Cell death normally removes supernumerary cells from the developing retina, and in *sevenless* degenerating cells are often observed near the site where the usurped cone cell normally rises.

Mutations effecting cell-specific transformations have also been described in *Drosophila* and in the nematode *Caenorhabditis elegans*. In *Drosophila*, the mutation *Hairless* causes cells normally fated to produce bristles to become socket-secreting cells instead (*12*). Mutations in the nematode gene *lin-12* can cause cells that normally follow divergent developmental pathways to adopt identical fates, leading to the duplication of certain structures and the absence of others (*13*).

When mutations act embryologically in *Drosophila*, large areas of tissue become developmentally transformed. Operating at the end of the determinative events in the fly's retina, *sevenless* causes only a single cell to switch its fate. Such an aberration occurring in this well-characterized cellular milieu offers an excellent opportunity to examine the machinery of a developmental decision.

REFERENCES AND NOTES

1. W. Bateson [*Materials for the Study of Variation* (Macmillan, London, 1894)] introduced the term "homeosis" to describe the phenomenon of "something changing into the likeness of something else." He cited numerous cases of homeosis, in examples ranging from flower petals to canine teeth.
2. E. B. Lewis, *Nature (London)* **276**, 565 (1978).
3. The *sevenless* allele used was sev^{LY5}, isolated by Seymour Benzer and co-workers in 1973. Until recently, this was the only known allele at the *sev* locus (1-33.2 ± 0.2). Five more alleles (sev^{d2}, sev^{f1}, sev^{f3}, sev^{x1}, and sev^{x3}) have now been isolated by F. Gerresheims (thesis, Faculty of Biology, Ludwig-Maximilians University of Munich, Munich, West Germany). To date, we have checked the f1, d2, and x1 alleles. *Sevenless* eyes were compared against Canton-S. and Massachusetts wild-type strains.
4. W. A. Harris, W. S. Stark, J. A. Walker, *J. Physiol. (London)* **256**, 415 (1976).
5. J. A. Campos-Ortega, G. Jurgens, A. Hofbauer, *Wilhelm Roux Arch. Entwicklungsmech. Org.* **186**, 27 (1979).
6. D. F. Ready, T. E. Hanson, S. Benzer, *Dev. Biol.* **53**, 217 (1976).
7. A. Tomlinson, *J. Embryol. Exp. Morphol.* **89**, 313 (1985).
8. M. S. Nowel and P. M. J. Shelton, *ibid.* **60**, 329 (1980).
9. P. A. Lawrence and S. M. Green, *Dev. Biol.* **71**, 142 (1979).
10. D. A. Weisblat and S. S. Blair, *ibid.* **101**, 326 (1984); S. L. Zackson, *ibid.* **104**, 143 (1984).
11. J. E. Sulston and J. G. White, *ibid.* **78**, 577 (1980).
12. A. D. Lees and C. H. Waddington, *Proc. R. Soc. London Ser. B* **131**, 87 (1942).
13. I. S. Greenwald, P. W. Sternberg, H. R. Horvitz, *Cell* **34**, 435 (1983).

14. We thank E. C. Cox, T. Tully, and E. Wieschaus for helpful comments on the manuscript. Supported by NSF grant BNS83-18235 and Sloan Foundation fellowship BR-2040.

12 August 1985; accepted 7 November 1985

Dynamics of Lymphocyte-Endothelial Interactions in Vivo

MATTHEW BJERKNES, HAZEL CHENG, CLIFFORD A. OTTAWAY

The dynamics of the attachment of lymphocytes to the endothelium of high endothelial venules in murine Peyer's patches were studied in vivo. Lymphocytes adhered readily to the endothelium lining these vessels, but most of the adhering cells detached within a few seconds. Many lymphocytes, however, experienced multiple collisions with the high endothelial venules, and this substantially increased the efficiency of lymphocyte collection by these vessels.

LYMPHOID TISSUES SUCH AS PEYER'S patches and lymph nodes routinely extract large numbers of blood-borne lymphocytes. The postcapillary venules of these lymphoid tissues have a specialized high endothelium to which lymphocytes adhere and then penetrate (*1*). For this to occur, a series of events must take place. First, the lymphocyte must arrive in the high endothelial venules (HEV) by way of the bloodstream and then collide with the endothelium. During this collision, the lymphocyte must adhere to the endothelium with sufficient tenacity to prevent it from being dislodged by hemodynamic forces. Furthermore, this attachment must occur at a site that permits penetration. Although the chance of a lymphocyte accomplishing all this would appear to be low, this is clearly not so.

Many specialized aspects of the anatomic and molecular basis of this unusual lymphocyte-endothelium interaction are understood (*2–13*). The dynamics of the process, however, have not been examined. We studied the interaction of fluorescently labeled lymphocytes with the endothelium of postcapillary venules of Peyer's patches in vivo, and we examined the dynamics of the lymphocyte attachment-detachment and collection processes in the HEV.

Peyer's patches bearing jejunal loops were exteriorized from female BALB/c mice anesthetized with pentobarbital (60 mg/kg). Postcapillary venules adjacent to follicles of the patches (Fig. 1) were visualized with an epifluorescence-equipped microscope. Single-cell suspensions of syngeneic mesenteric lymph-node lymphocytes were labeled with tetramethylrhodamine isothiocyanate

M. Bjerknes and H. Cheng, Department of Anatomy, Medical Sciences Building, University of Toronto, Ontario, Canada, M5S 1A8.
C. A. Ottaway, Department of Medicine, St. Michael's Hospital, University of Toronto, Ontario, Canada, M5S 1A8.